Materials Science & Engineering A 597 (2014) 89–94

Contents lists available at ScienceDirect

Materials Science & Engineering A

journal homepage: www.elsevier.com/locate/msea

Capturing the stochastic mechanical behavior of micro and nanopillars

Avraam A. Konstantinidis [a], Katerina E. Aifantis [a,b,*], Jeff Th.M. De Hosson [c]

[a] Lab of Mechanics & Materials, Aristotle University of Thessaloniki, Thessaloniki 54124, Greece
[b] Civil Engineering, University of Arizona, Tucson, AZ 85721, USA
[c] Applied Physics, University of Groningen, Groningen 9747AG, The Netherlands

ARTICLE INFO

Article history:
Received 1 November 2013
Accepted 13 December 2013
Available online 22 December 2013

Keywords:
Micropillars
Nanopillars
Cellular automaton
Gradient plasticity
Stochastic

ABSTRACT

Experimental evidence has illustrated that micropillar deformation is highly stochastic, as the stress–strain curves are manifested by multiple strain bursts. Although initial theoretical works employing gradient plasticity can predict the stress–strain response of individual pillars, they cannot capture the stochastic effects observed for multiple same diameter specimens. This article presents simulations that are not only in precise qualitative and quantitative agreement with experimental stress–strain curves for varying diameter pillars, but can also account for the observed stochasticity in same diameter micropillars. This is accomplished by implementing gradient plasticity within a cellular automaton, while allowing the yield-stress to randomly vary within the micropillar. In concluding, it is shown that the aforementioned numerical code can also capture the stress drops and size dependent strengthening observed in metallic glass nanopillars.

1. Introduction

The stress–strain response of micropillars during compression is characterized by significant stochastic effects, which are manifested through multiple strain bursts [1–10]. The stress–strain curves for same diameter pillars differ significantly, however, they can be enclosed within bounds, and therefore a size effect is noted [1–4]. Such size effects can be attributed to the significant dislocation activity and corresponding evolution of strain gradients that take place during compression, as documented by in-situ microdiffraction experiments [7–9]. Deformation characteristics of pillars such as slip zones are also observed through scanning electron microscopy (SEM) [1,2,10,11].

In order, hence, for a theoretical model to interpret micropillar compression, it should be able to account for the aforementioned microstructural characteristics: strain gradients and slip zones. The authors of [12] accounted for such slip zones by dividing the micropillar into layers (along the *y*-direction), which yielded consecutively (each zone was characterized by its own yield stress). The resulting boundary value problem was then solved using gradient plasticity [13–15] and strain bursts were predicted when two adjacent layers were deforming plastically. The theoretical predictions were in very good agreement with the experimental data of [1], since precise fits could be obtained, but stochastic effects that are inherent to micropillar deformation were not accounted for. Since, however, stochasticity is a main characteristic of pillar deformation, it is necessary to employ appropriate numerical models that can predict statistically different stress–strain curves for same diameter pillars. As a first step Monte Carlo (MC) simulations were used in [3,4] to develop bounds that could enclose the scattered stress–strain response of same diameter Al micropillars, however, quantitative agreement with the experimental curves was not obtained, and the MC approach cannot account for the underlying microstructure. A step closer towards capturing the stochastic response of same diameter pillars was achieved in [16], where the model of [12] was successfully applied for bounding the stress–strain response of numerous 6 μm and 2 μm Al pillars.

The novelty of the present contribution concentrates on the numerical implementation of the constitutive gradient plasticity model of [12]. It will be shown in the sequel that the stochastic effects observed in the stress–strain behavior of micropillars are successfully captured by implementing the gradient formulation of [12] in a cellular automaton and using a stochastic term to characterize the yield stress of each layer that the pillar is divided into. Essentially this allows the yield stress to vary throughout the pillar. The model is illustrated by relating the simulation predictions directly to the experimental stress–strain curves for 4.9 μm diameter Ni micropillars (Fig. 1).

In this connection, it should be noted that prior to the successful application of gradient plasticity in interpreting micropillar compression, several other theories had been proposed to explain this size-dependent strengthening, and no agreement on

* Corresponding author at: 1209 E. Second Street, Tucson, AZ 85721, USA. Tel.: 520 621 2266.
E-mail address: aifantis@email.arizona.edu (K.E. Aifantis).

0921-5093/$ - see front matter © 2013 Elsevier B.V. All rights reserved.
http://dx.doi.org/10.1016/j.msea.2013.12.053

postulating a unified plasticity theory had emerged [2]. The two prominent deformation mechanisms that had been proposed were single-arm source theory [17–19] and dislocation starvation followed by surface nucleation first proposed in [20] and subsequently corroborated by atomistic simulations in [21–24]. In the former, the formation of dislocations occurs by the operation of "partial Frank–Read sources", or truncated sources, single-arm sources, and in the latter by surface nucleation of dislocations once all the pre-existing mobile dislocations have annihilated at the free pillar surface. While these theories may appear to be competing, it is likely that they both take place at different pillar sizes: with single-arm sources strengthening occurring in the micron-sized pillars down to 100 nm and with dislocation starvation followed by surface nucleation prevailing at the smaller sizes, deep in the sub-micron regime (below 50 nm).

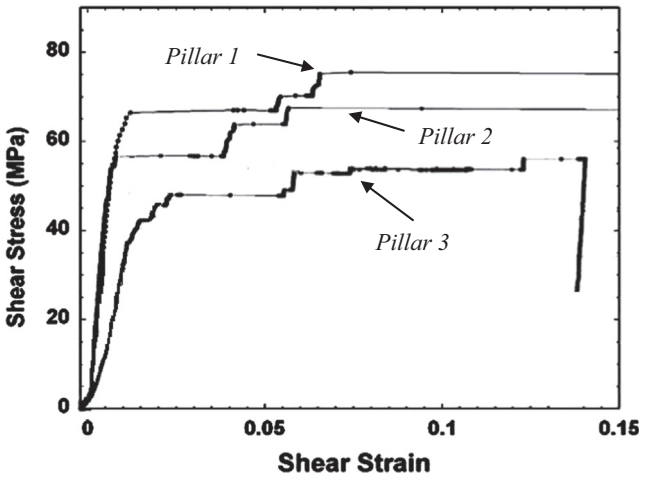

Fig. 1. Experimental stress–strain curves of Ni micropillars of 4.9 μm diameter [1].

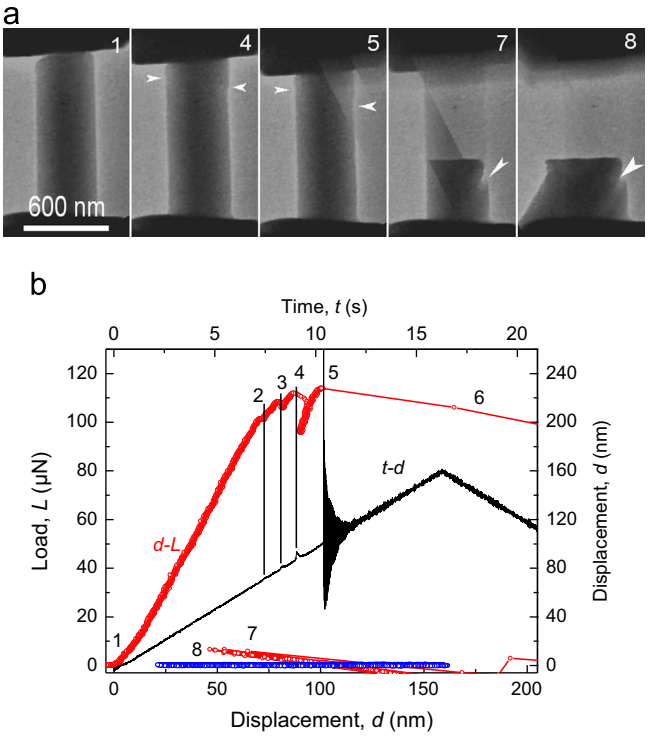

Fig. 2. (a) Video frames recording the deformation of a ⌀490 nm $Al_{86}Ni_9Y_5$ MG taper-free pillar compressed under displacement-control mode in a SEM. Grabbed video frames (1–8) show the deformation structures before, during and after compression (white filled arrows indicate the shears). (b) Load–displacement and time–displacement curves with the vertical black lines (2–5) indicating shear events. Line 5 corresponds to the time and displacement when pillar has been broken. The numbers on the *d*–*L* curve correspond to the numbers of video frames.

Hence, in concluding this work, it will be shown that the proposed numerical implementation of gradient plasticity can also capture the stochastic stress–strain response of metallic glass (MG) $Zr_{50}Ti_{16.5}Cu_{15}Ni_{18.5}$ nanopillars [10], with diameters of 410 nm and 112 nm. Fig. 2 illustrates the formation of shear bands in an $Al_86Ni_9Y_5$ MG nanopillar during compression. It can be seen that stress drops occurred during the development of shear bands, while upon fracture of the pillar a plateau took place. This shear band formation indicates the formation of slip zones within nanopillars during compression, similar to those noted in micropillars.

The behavior Cu-, Zr-, Al-MG based pillars does not differ much, aside from the ductility of Al-based MGs being much higher compared to the rest, for diameters below 320 nm. Hence, based on the experimental evidence shown in Fig. 2, when modeling MG-nanopillars above 100 nm, it can be assumed that the pillar can be divided into layers as the micropillars are. The stochasticity can be seen in the stress–strain curves (e.g. Fig. 2b) for individual nanopillars, since multiple stress drops occur throughout compression. Furthermore, size-dependent strengthening has also been observed as the diameter decreases. Hence in the present article it will be shown how gradient plasticity implemented in a cellular automaton simulation can capture both the stochastic effects in the stress–strain curves, and also the size-dependent hardening observed in metallic glass nanopillars that are above 100 nm. This is the first time that gradient plasticity is applied for nanopillar deformation modeling.

2. Modeling micropillar stochasticity

For a material that is characterized by linear hardening after yielding, a deformation theory version of gradient plasticity leads to the constitutive differential equation [12]

$$\begin{cases} \overline{\sigma} = E\varepsilon & \text{for} \quad \varepsilon \le \sigma^y/E, \\ \beta\ell^2\frac{\partial^2\varepsilon^p}{\partial x^2} - \beta\varepsilon^p + \overline{\sigma} - \sigma^y = 0 & \text{for} \quad \varepsilon > \sigma^y/E, \end{cases} \tag{1}$$

where ε^p is the plastic strain, E is the elastic modulus, β is the hardening modulus, $\overline{\sigma}$ and σ^y are the applied and yield stress, respectively, and ℓ is the corresponding internal length, which is a material parameter that comes into play in all gradient theories and characterizes the underlying microstructure. In these micropillar experiments, the initial portion of the stress–strain curves in Fig. 1 may not be completely elastic, due to slippage and friction occurring between the pillar (free on one end) and the indenter. In applying, therefore, this formulation to micropillars, E does not correspond to the actual modulus of elasticity, but to an effective modulus, which is given by the slope of the initial curves in the stress–strain graphs; i.e. it is the slope of the elastic region, before any yielding occurs in the pillar.

A schematic representation of the pillar division into layers, in order to capture the slip zones, is shown in Fig. 3. In the theoretical model of [12] the top and bottom layers were taken to deform elastically, while the gauge region was allowed to deform plastically through sequential yielding of the adjacent discrete slip zones. However, according to experimental evidence [25] slip traces and slip lines do not develop sequentially, at adjacent regions, but "inhomogeneously" depending on the nucleation and propagation conditions of dislocations. Hence, in the present implementation all layers in the pillar are allowed to deform plastically, and their yielding occurs in a random order. Strain